



Both Transmembrane Domains of BK β 1 Subunits Are Essential to Confer the Normal Phenotype of β 1-Containing BK Channels

Guruprasad Kuntamallappanavar¹, Ligia Toro², Alex M. Dopico^{1*}

1 Department of Pharmacology, College of Medicine, The University of Tennessee Health Science Center, Memphis, Tennessee, United States of America, **2** Departments of Anesthesiology and of Molecular and Medical Pharmacology, University of California Los Angeles, David Geffen School of Medicine, Los Angeles, California, United States of America

Abstract

Voltage/ Ca^{2+} -gated, large conductance K^+ (BK) channels result from tetrameric association of α (slo1) subunits. In most tissues, BK protein complexes include regulatory β subunits that contain two transmembrane domains (TM1, TM2), an extracellular loop, and two short intracellular termini. Four BK β types have been identified, each presenting a rather selective tissue-specific expression profile. Thus, BK β modifies current phenotype to suit physiology in a tissue-specific manner. The smooth muscle-abundant BK β 1 drastically increases the channel's apparent Ca^{2+} sensitivity. The resulting phenotype is critical for BK channel activity to increase in response to Ca^{2+} levels reached near the channel during depolarization-induced Ca^{2+} influx and myocyte contraction. The eventual BK channel activation generates outward K^+ currents that drive the membrane potential in the negative direction and eventually counteract depolarization-induced Ca^{2+} influx. The BK β 1 regions responsible for the characteristic phenotype of β 1-containing BK channels remain to be identified. We used patch-clamp electrophysiology on channels resulting from the combination of smooth muscle slo1 (cbv1) subunits with smooth muscle-abundant β 1, neuron-abundant β 4, or chimeras constructed by swapping β 1 and β 4 regions, and determined the contribution of specific β 1 regions to the BK phenotype. At Ca^{2+} levels found near the channel during myocyte contraction (10 μM), channel complexes that included chimeras having both TMs from β 1 and the remaining regions ("background") from β 4 showed a phenotype (V_{half} , τ_{act} , τ_{deact}) identical to that of complexes containing *wt* β 1. This phenotype could not be evoked by complexes that included chimeras combining either β 1 TM1 or β 1 TM2 with a β 4 background. Likewise, β "halves" (each including β 1 TM1 or β 1 TM2) resulting from interrupting the continuity of the EC loop failed to render the normal phenotype, indicating that physical connection between β 1 TMs *via* the EC loop is also necessary for proper channel function.

Citation: Kuntamallappanavar G, Toro L, Dopico AM (2014) Both Transmembrane Domains of BK β 1 Subunits Are Essential to Confer the Normal Phenotype of β 1-Containing BK Channels. PLoS ONE 9(10): e109306. doi:10.1371/journal.pone.0109306

Editor: Stuart E Dryer, University of Houston, United States of America

Received: August 1, 2014; **Accepted:** September 10, 2014; **Published:** October 2, 2014

Copyright: © 2014 Kuntamallappanavar et al. This is an open-access article distributed under the terms of the Creative Commons Attribution License, which permits unrestricted use, distribution, and reproduction in any medium, provided the original author and source are credited.

Data Availability: The authors confirm that all data underlying the findings are fully available without restriction. All relevant data are within the paper itself.

Funding: This work is supported by R37 AA11560 (AMD) from the National Institute on Alcohol Abuse and Alcoholism, www.niaaa.nih.gov, R01 HL104631 (AMD) from the National Heart, Lung, and Blood Institute, www.nhlbi.nih.gov, Predoctoral Fellowship (GK) from the American Heart Association, www.aha.org, and R01 HL107418 (LT) from the National Heart, Lung, and Blood Institute, www.nhlbi.nih.gov. The funders had no role in study design, data collection and analysis, decision to publish, or preparation of the manuscript.

Competing Interests: Alex Dopico is currently a PLOS ONE Editorial Board Member. This does not alter the authors' adherence to PLOS ONE Editorial policies and criteria.

* Email: adopico@uthsc.edu

Introduction

Large conductance, voltage- and Ca^{2+} -gated K^+ (BK) channels are ubiquitously expressed and thus, control numerous physiological processes [1–3]. Functional BK channels result from tetrameric association of channel-forming proteins termed α (slo1) subunits. These subunits contain a transmembrane S1-S6 region that is primarily responsible for ion permeation and voltage-gating, and conserved in all members of the TM6 superfamily of voltage-gated K^+ (K_V) channels. In addition, slo1 proteins distinctively contain: 1) a transmembrane (TM) segment S0 that leads to an extracellular N-end [4], which participates in voltage-sensing [5–7], and 2) a large cytosolic C-end (CTD), which allows the BK channel to increase activity in response to increased Ca^{2+} within the physiological range [8] (**Fig. 1**).

In most tissues, however, slo1 is associated with accessory proteins termed β subunits. Several BK β subunit-coding sequences have been cloned (β 1– β 4), all their protein products sharing a common design: short intracellular (IC) N- and C-ends and two TMs (TM1, TM2) connected by an extracellular (EC) loop (**Fig. 1**). Remarkably, BK β subunit type expression is highly tissue-specific, and the modification in slo1 current introduced by a given β type helps to define channel phenotypes that suit cell physiology in a tissue-specific manner [2,9]. BK β 1 subunit abundant expression in smooth muscle (SM) results in a robust increase in the native channel's apparent Ca^{2+} sensitivity. Therefore, SM BK channels drastically increase activity when slo1 sensors are exposed to changes in Ca^{2+} from the sub- μM levels found under resting conditions to \sim 4–30 μM , these levels being reached in the vicinity of the BK channel's Ca^{2+} sensors in

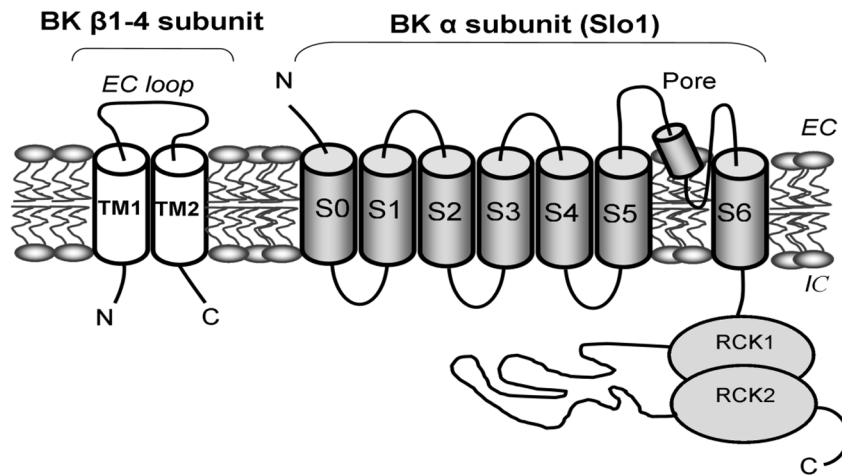


Figure 1. Schematic structure of β 1 subunit-containing BK channel. Cartoon showing a slo1- β 1 subunit heterodimer. The channel-forming slo1 subunit includes transmembrane (TM) segments S0-S6 and intracellular Regulatory of Conductance for K^+ (RCK) domains, these domains including distinct residues that participate in sensing changes in Ca^{2+}_i . Four slo1 monomers assemble to render fully functional BK channels. All four types of β subunits identified so far contain a similar design that includes intracellular N- and C-terminals, two transmembrane domains (TM1 and TM2), and an EC loop. EC and IC correspond to the extracellular and intracellular sides of the membrane.
doi:10.1371/journal.pone.0109306.g001

the contracting SM cell [10]. The resulting hyperpolarizing outward K^+ currents generated by β 1-containing BK channels negatively feed-back on Ca^{2+}_i increase and thus, limit SM contraction [11].

The increase in channel's apparent Ca^{2+}_i sensitivity induced by BK β 1 results from complex regulation of slo1 gating by this regulatory subunit, including modulation of Ca^{2+}_i -channel protein interaction itself and voltage-sensor activation [1,12,13], and reduction in voltage-dependence steepness [14–16]. BK β 1 subunits, however, decrease channel activity at sub- μ M Ca^{2+}_i by reducing intrinsic gating (i.e., the capability of the channel to gate in absence of voltage-activation, Ca^{2+}_i -binding or any other regulator) [1,13]. BK β 1 also slows activation and deactivation kinetics [15,17] and participates in channel sensitivity to 17β -estradiol [18] and cholane steroids and non-steroidal analogs [19,20]. While the changes in BK channel phenotype introduced by β 1 have been studied in detail, identification of the specific BK β 1 regions that participate in determining the characteristic β 1-containing BK channel phenotype remains unresolved.

Data from msl01/dslo chimeras seem to indicate that the region expanding from the N-end to the S0-S1 loop contributes to modulation of apparent Ca^{2+}_i sensitivity by β 1 or β 2 subunits [21]. Cysteine disulfide cross-linking studies attribute to the EC sides of β 2, β 3, and β 4 TM1 and TM2 topological associations with slo1 that are similar to those of β 1 EC sides [22,23]. In spite of these proposed topological similarities, ion channel current phenotypes resulting from heteromeric association between slo1 and each β type differ markedly [reviewed in 9]. Moreover, neither cysteine substitutions *per se* nor disulfide cross-linking in EC regions have major effects on several key parameters of BK ionic current phenotype such as current half-voltage activation (V_{half}), activation or deactivation kinetics [5], strongly suggesting that regions non-accessible to cysteine substitutions (e.g., TMs) could play a key role in determining the phenotype of β 1-containing BK channels. Consistent with this possibility, β 1 EC loop Ala substitutions that altered some gating parameters failed to eliminate the characteristic leftward-shift along the voltage axis introduced by β 1 [24]. On the other hand, functional studies from BK channels made of slo1 and chimeric β 1/ β 2 subunits indicate that β C- and N-ends

play a significant role in determining the channel phenotype, yet a shared modulatory role by TMs has been hypothesized [16].

To determine whether BK β 1 TM1, TM2 or both are critical to provide the characteristic ion current phenotype of BK β 1-containing BK channels, we combined surface protein biotinylation assays with patch-clamp studies under wide voltage and Ca^{2+}_i ranges (which included the values found in the SM myocyte under physiological conditions) on heteromeric BK complexes resulting from the association of rat cerebral artery SM slo1 (“cbv1”) with engineered BK β 1. Using this approach, we demonstrate that: 1) neither TM is sufficient but both are necessary to establish the characteristic phenotype of BK β 1-containing BK channels, and 2) physical connection between both TMs *via* the EC loop is necessary to maintain such phenotype. This information is important to begin to understand the unique role of BK β 1 in regulating channel function and cell physiology, and for future rationale design of ligands that selectively target β 1-containing BK channels.

Experimental Procedures

Ethics statement

Care of animals and experimental protocols (internal protocol #1078) were reviewed and approved by the Institutional Animal Care and Use Committee at the University of Tennessee Hlth. Sci. Ctr., which is an Association for Assessment and Accreditation of Laboratory Animal Care-accredited institution (A3325-01; 07/10/2012-07/31/2016).

cRNA preparation and injection into *Xenopus laevis* oocytes

Cloning, expression and functional characterization of cbv1 (AY330293) are provided elsewhere [25,26]. BK h β 1, h β 4, and h β 1/h β 4 chimeric cDNAs (β 1TMs₄, β 4TMs₁, β 4TM1₁ and β 4TM2₁) were cloned in Dr. Ligia Toro's lab (UCLA). In addition, we engineered two “split” chimeras from the β 4TMs₁ to render: 1) “N-half chimera”, which contained the N-terminus from β 4, TM1 from β 1 and proximal half of β 4 EC loop; 2) “C-half chimera”, which contained the distal half of β 4 EC loop, TM2

from $\beta 1$, and the C-terminus from $\beta 4$. Flag tag was inserted at N-terminus of C-half chimera to detect during surface biotinylation. All constructs were verified by automated sequencing (Molecular Resource Center, University of Tennessee Health Science Center). These cDNAs were subcloned into pOx for oocyte expression.

cRNA was dissolved in diethyl polycarbonate-treated water at 10 (cbv1) and 30 ($\beta 1$) ng/ μ l; 1 μ l aliquots were stored at -70°C . Oocytes were removed from *Xenopus laevis* (Xenopus Express), prepared and cRNA-injected as described [27]. The interval between injection and patch-clamping was ≥ 36 h.

Electrophysiology

Oocytes were prepared for patch-clamp electrophysiology as previously described [27], with Inside out (I/O) patches being used to record macroscopic ion current. Bath and electrode solutions contained (mM): 130 K-gluconate, 5 EGTA, 1.6 HEDTA, 15 HEPES; pH 7.4. Variant amounts of CaCl_2 and MgCl_2 were used to set the free Ca^{2+} at the desired level and free Mg^{2+} to 1 mM. Free Ca^{2+} and Mg^{2+} were calculated using Max Chelator (C. Patton; Stanford). Actual Ca^{2+} levels in solution were determined experimentally with Ca^{2+} -sensitive electrodes (Corning) [27]. For experiments in nominal zero Ca^{2+}_i , EDTA was substituted by 5 mM EGTA and no Ca^{2+} was added to the recording solutions. Free $[\text{Ca}^{2+}]$ in this nominal zero Ca^{2+}_i solution is 0.5 nM [21]. In the experiments where the free Ca^{2+} was set to $< 1 \mu\text{M}$, 1.6 mM HEDTA was omitted from the solution. All chemicals were purchased from Sigma.

Patch electrodes were pulled from glass capillaries (Drummond). The procedure gave tip resistances of 3–5 M Ω when filled with electrode solution. Experiments were carried out at room temperature (21°C). BK currents were acquired using an EPC8 (HEKA Electronics) amplifier and digitized using Digidata 1320A-pCLAMP8 (Molecular Devices). Macroscopic currents were evoked from a holding potential of -80 mV by 100 ms-long, 10 mV depolarizing steps from -150 to $+150$ – 200 mV. Standard P/4 leak subtraction routine was applied using a built-in function in pCLAMP. Currents were low-pass filtered at 1 kHz and sampled at 5 kHz.

Conductance-Voltage (G-V) relations were determined from the tail current amplitude, as described [15]. Resulting $G/G_{\text{max}}-V$ plots were fitted to a Boltzmann function of the type $G(V) = G_{\text{max}} / (1 + \exp[-(V + V_{1/2})/k])$. Boltzmann fitting routines were run using the Levenberg-Marquardt algorithm to perform nonlinear least squares fits. Macroscopic current activation and deactivation data were fitted to standard exponential functions using a Chebyshev approximation. Time constant for current activation (τ_{act}) was measured at the voltage at which the channel reached maximal steady-state activity (V_{max}) while deactivation time constant (τ_{deact}) was measured after voltage reached V_{max} and then stepped down to -80 mV [17]. Data fitting and plotting were performed using Clampfit 9.2 (Molecular Devices) and Origin 8.5 (OriginLab).

Detection of N-half and C-half chimeric proteins on the cell membrane surface by biotinylation

Presence of N-half and C-half chimeric proteins on the membrane surface of *Xenopus laevis* oocytes was detected using the Pierce Cell Surface Protein Isolation kit (Thermo Scientific) following the manufacturer's instructions. Immediately prior to the biotinylation-based labeling and separation of membrane surface proteins, the oocyte's follicular layer was removed to allow access of kit reagents to the cell membrane. The purified surface protein fraction was analyzed by Western blotting.

Western blotting

Purified surface protein fraction for biotinylation (30 $\mu\text{g}/\text{lane}$) was separated on a 4–15% SDS-polyacrylamide gel and transferred onto PVDF (polyvinylidene difluoride) membranes. The membranes were then blocked with 5% non-fat dry milk made in tris-buffered saline containing 0.1% Tween 20 for 2 hrs. Membranes were then incubated with appropriate primary antibodies overnight at 4°C in Tris-buffered saline (TBS) with 0.1% Tween 20 (TBS-T) and 5% nonfat dry milk. Membranes were then incubated with appropriate horseradish peroxidase-conjugated secondary antibodies (1:10,000 dilution; Milipore) for 1–2 hrs at room temperature. Proteins were then visualized using SuperSignal West Pico Chemiluminescent Substrate kit (Thermo Fisher Scientific). A slo1 $\beta 4$ antibody (1:200 dilution; Alamone) was used to recognize the N-terminus of $\beta 4$ subunit, and a mouse monoclonal anti-FLAG M2 antibody (1:200 dilution; Sigma Aldrich) was used to detect the C-half chimera.

Statistics

Analysis was performed using InStat 3.0 (GraphPad). Data were analyzed with one-way ANOVA followed by Tukey's multiple comparison test [28]. Significance was set at $P < 0.05$. Data are expressed as mean \pm SEM; n = number of patches, each patch obtained from a separate oocyte.

Results

$\beta 1$ TMs regulate BK current phenotype

When considering all BK β subunit types, primary alignment of $\beta 1$ vs. $\beta 4$ reveals the highest number (56%) of non-identical and non-conserved residues [17]. Moreover, $\beta 1$ vs. $\beta 4$ co-expression with slo1 proteins renders BK channels with a different phenotype: noteworthy, $\beta 1$ subunits greatly increase the apparent Ca^{2+} sensitivity of the channel at Ca^{2+}_i concentrations $> 1 \mu\text{M}$ whereas the $\beta 4$ subunit effect is rather limited, requiring $\geq 30 \mu\text{M}$ Ca^{2+}_i to be observed [1,15,17]. Thus, we used chimeras resulting from swapping h $\beta 1$ /h $\beta 4$ TM regions (whether individually or two at a time) to determine the contribution of $\beta 1$ TMs to the $\beta 1$ -containing BK channel phenotype. These $\beta 1/\beta 4$ chimeras have been routinely used in our laboratory, their surface expression and function being confirmed by pharmacological profiling as described elsewhere [29]. Macroscopic ionic BK currents mediated by cbv1 \pm h β (*wt* $\beta 1$, *wt* $\beta 4$ or $\beta 1/\beta 4$ chimeras) were evoked by depolarizing steps (Materials and Methods) from inside-out (I/O) macropatches exposed to a wide Ca^{2+}_i range (nominal zero– $100 \mu\text{M}$). This range includes the Ca^{2+}_i faced by BK Ca^{2+} -sensors that is required for cerebrovascular SM BK channels to fulfill their physiological role, that is, negatively feedback on depolarization-induced Ca^{2+} entry and SM contractility [4– $30 \mu\text{M}$; 10]. To identify the ion channel phenotype of the resulting BK channel complexes, we obtained $G/G_{\text{max}}-V$ plots, τ_{act} and τ_{deact} from each macropatch (ionic current traces shown in **Fig. 2A**). The time constants τ_{act} and τ_{deact} are widely recognized as indicators of BK current kinetics while $G/G_{\text{max}}-V$ plots were obtained to extrapolate V_{half} . This parameter is indicator of overall BK channel activity, including both Ca^{2+}_i -dependent and Ca^{2+}_i -independent gating components [15,30].

As shown for other slo1 channels [16,17,31], co-expression of h $\beta 1$ with cbv1 markedly left-shifted the $G/G_{\text{max}}-V$ plot along the voltage axis, leading to a ~ 50 mV decrease in V_{half} at physiological, $10 \mu\text{M}$ Ca^{2+}_i : $V_{\text{half}} = 21.42 \pm 2.39$ and -33.22 ± 3.56 mV for cbv1 and cbv1+h $\beta 1$, respectively ($P < 0.05$) (**Figs. 2B,C and S1A**). Consistent with previous studies [16,17,31], the h $\beta 1$ -driven shift in V_{half} increased as Ca^{2+}_i was raised above $\sim 1 \mu\text{M}$ (**Fig.**

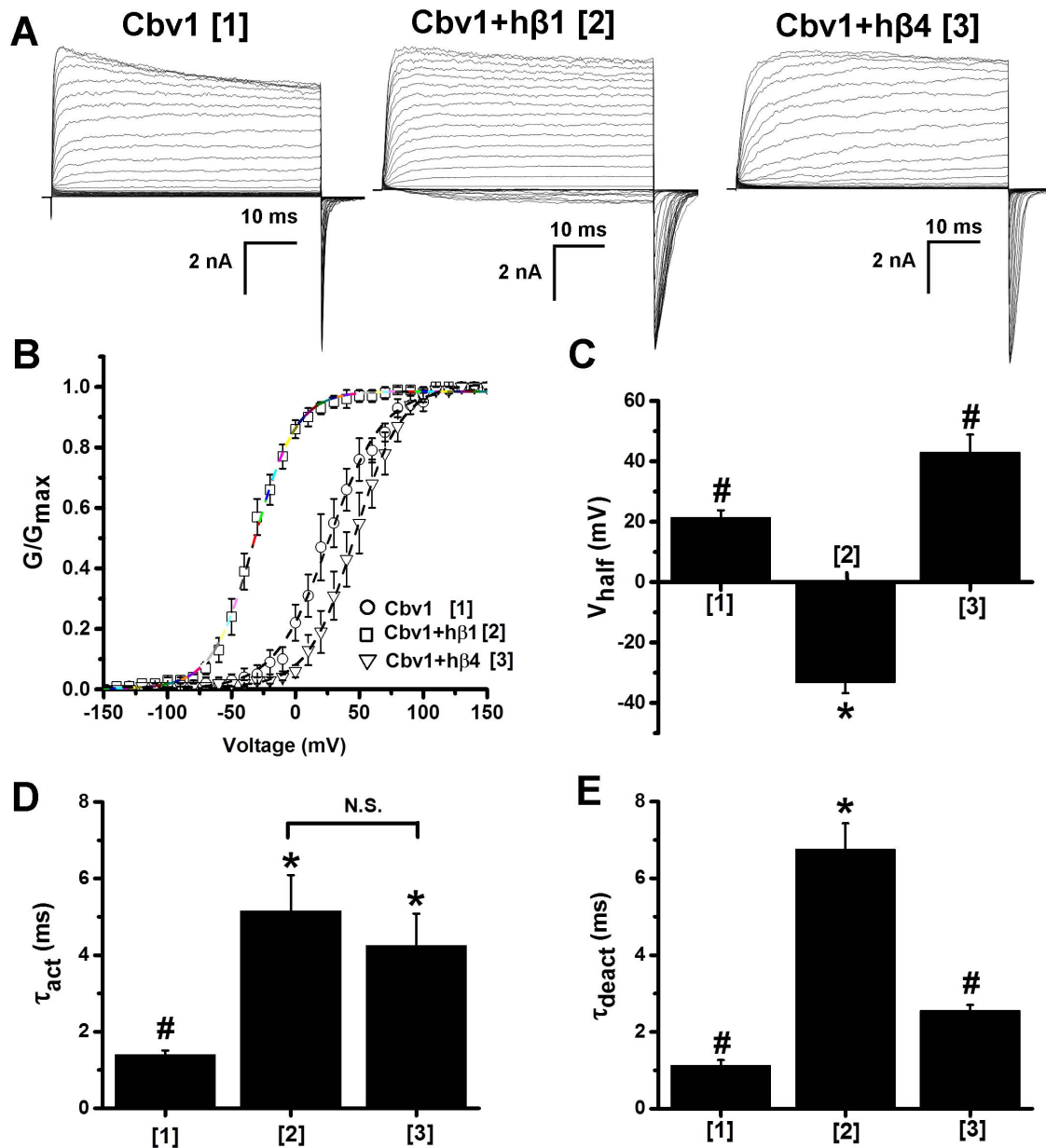


Figure 2. Characteristic BK current phenotype of channels made of $cbv1 \pm \beta$ 1 or β 4 subunits. Representative traces of macroscopic current recordings and averaged G/G_{max} - V plots (B) obtained from I/O oocyte membrane patches expressing $cbv1$ (construct 1), $cbv1+h\beta1$ (construct 2) or $cbv1+h\beta4$ (construct 3); $Ca^{2+}_i = 10 \mu M$. Bar graphs show averaged V_{half} (C), activation (D) and deactivation (E) time constants (τ_{act} , τ_{deact} , respectively) obtained for $cbv1$, $cbv1+h\beta1$, and $cbv1+h\beta4$; $Ca^{2+}_i = 10 \mu M$. *Different from $cbv1$ ($P < 0.05$); #Different from $cbv1+h\beta1$ ($P < 0.05$). Error bars correspond to SEM; each point represents the average of ≥ 4 patches. doi:10.1371/journal.pone.0109306.g002

S1A). Results underscore that μM Ca^{2+}_i levels, while not necessary (**Figs. 2BC and S1A**), are optimal for β 1-modulation of $slo1$, this modulation resulting in increased apparent Ca^{2+} sensitivity and thus enhanced steady-state current [12,14,15,32]. In addition to its effect on $cbv1$ current V_{half} , $h\beta1$ remarkably increased τ_{act} and τ_{deact} : at $10 \mu M$ Ca^{2+}_i , τ_{act} and τ_{deact} changed from 1.40 ± 0.10 and 1.13 ± 0.13 ms to 5.16 ± 0.93 and 6.76 ± 0.67 ms, for $cbv1$ and $cbv1+h\beta1$, respectively ($P < 0.05$ for both constants) (**Fig. 2D,E**). These changes are also in agreement with data from $\beta1 \pm slo1$ other than $cbv1$ documenting a slowing down of macroscopic current activation and deactivation kinetics by BK β 1 subunits [12,15,17].

In contrast to $h\beta1$, $h\beta4$ expression increased $cbv1$ V_{half} at 0.3 – $10 \mu M$ Ca^{2+}_i while mildly decreasing V_{half} at 30 – $100 \mu M$ Ca^{2+}_i (**Fig. 2B,C and S1A**). At $10 \mu M$ Ca^{2+}_i , $h\beta4$ markedly increased τ_{act} : 1.40 ± 0.1 ms in $cbv1$ vs. 4.25 ± 0.83 ms in $cbv1+h\beta4$ ($P < 0.05$), and exerted a mild effect on τ_{deact} (**Fig. 2D,E**). Collectively, the β 4-introduced changes in V_{half} , τ_{act} and τ_{deact} over $cbv1$ values are similar to those reported with β 4 and other $slo1$ s [9,17].

We next co-expressed $cbv1$ with chimeric β 1TMs $_4$ subunits that contained $h\beta4$ TMs on $h\beta1$ “background” (i.e., $h\beta1$ EC loop and IC ends; **Fig. 3A**). $cbv1$ channels co-expressed with these chimeras displayed V_{half} - Ca^{2+}_i plots, τ_{act} and τ_{deact} that matched those of $cbv1+h\beta4$ ($P > 0.05$) while differing from those of $cbv1+h$

h $\beta 1$ (Figs. 3C-F and S1B). Conversely, cbv1+chimeric $\beta 4$ TMs₁ that contained h $\beta 1$ TMs introduced to an h $\beta 4$ background (Fig. 3A), showed a phenotype that matched that of cbv1+h $\beta 1$: $V_{\text{half-Ca}^{2+}_i}$ plot across all Ca^{2+}_i tested (0.3–100 μM ; Fig 3B-D and S1B), τ_{act} (Fig 3E) and τ_{deact} (Fig 3F) were all similar to those from cbv1+h $\beta 1$ ($P > 0.05$). These results indicate that $\beta 1$ TMs (but not the $\beta 1$ background) are critical to support the major characteristics of steady-state ionic current generated by $\beta 1$ -containing BK protein complexes.

To identify whether a particular BK $\beta 1$ TM was sufficient to determine the h $\beta 1$ -containing BK channel phenotype, we next engineered h $\beta 1$ /h $\beta 4$ chimeras that contained either TM1

($\beta 4$ TM1₁) or TM2 ($\beta 4$ TM2₁) from h $\beta 1$ introduced onto a $\beta 4$ background, and thus co-expressed such constructs with cbv1 channels (Fig. 4A). $V_{\text{half-Ca}^{2+}_i}$ plots (Fig. 4C,D and S1C) and τ_{deact} (Fig. 4F) from the resulting cbv1+chimeric $\beta 1/\beta 4$ heteromers drastically differed from those of cbv1+h $\beta 1$. Likewise, τ_{act} from $\beta 4$ TM1₁ was significantly different from that of cbv1+h $\beta 1$, with $\beta 4$ TM2₁ τ_{act} reaching intermediate values (Fig. 4E). Therefore, in contrast to $\beta 4$ TMs₁ containing both TM segments of $\beta 1$, $\beta 4$ TM1₁ and $\beta 4$ TM2₁ that contained only one of the TM of $\beta 1$ failed to substitute for h $\beta 1$ in characteristically modifying the cbv1 channel phenotype. Therefore, both $\beta 1$ TMs are required to render the phenotype characteristic of cbv1+h $\beta 1$ channels.

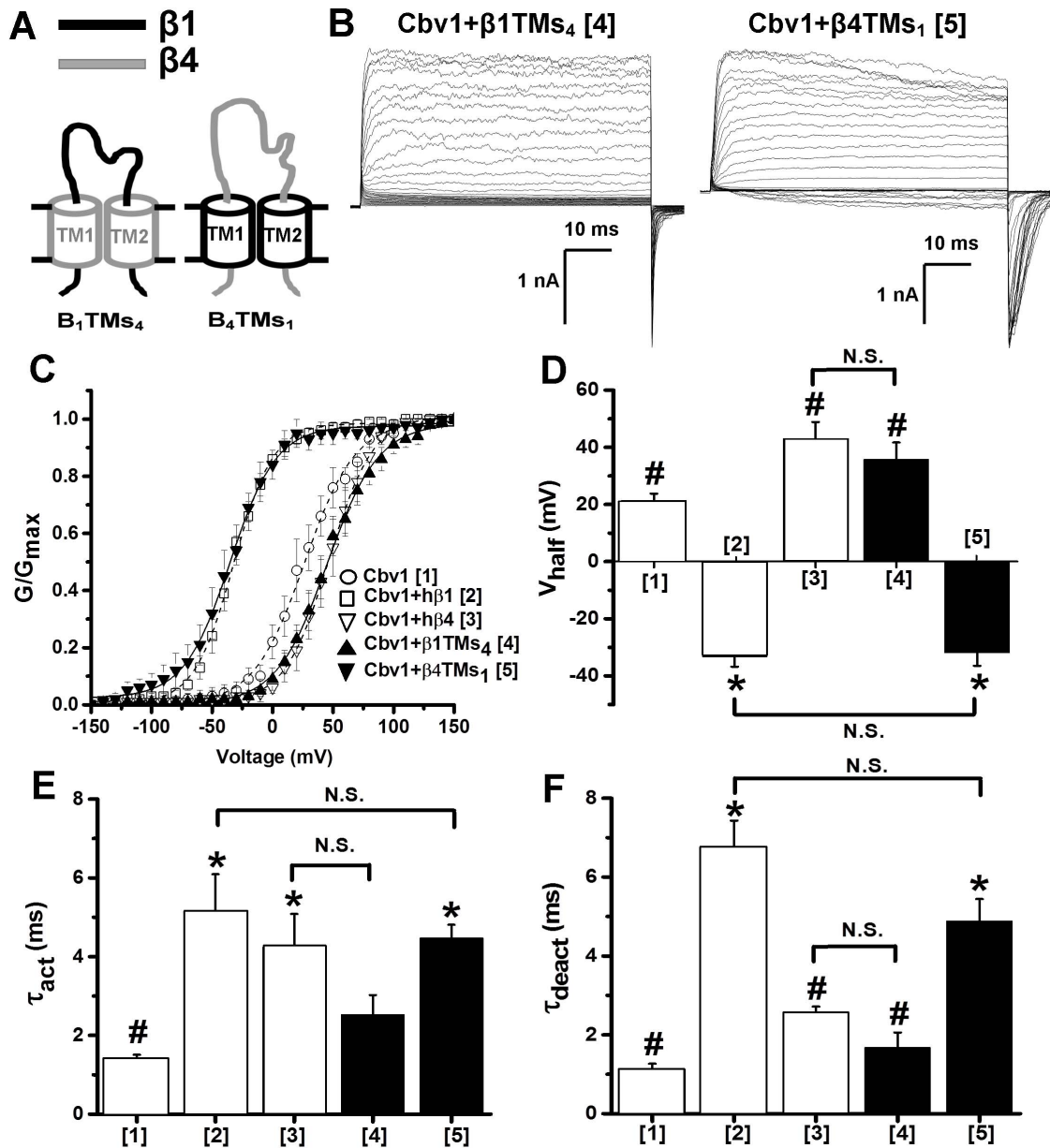


Figure 3. Both TMs of $\beta 1$ are required for conferring the characteristic phenotype of $\beta 1$ -containing BK channel complexes. (A) Cartoons depicting the chimeric constructs obtained by swapping TM protein regions between h $\beta 1$ and h $\beta 4$ subunits. Regions from $\beta 1$ and $\beta 4$ are given in black and grey, respectively. (B) Macroscopic current recordings obtained from I/O oocyte membrane patches expressing cbv1+ $\beta 1$ TMs₄ (construct 4) and cbv1+ $\beta 4$ TMs₁ (construct 5) $\text{Ca}^{2+}_i = 10 \mu\text{M}$. (C) Averaged $G/G_{\text{max}}-V$ plots of constructs 1–5 obtained at $\text{Ca}^{2+}_i = 10 \mu\text{M}$. Averaged V_{half} (D), activation (E) and deactivation (F) time constants (τ_{act} , τ_{deact} , respectively) from constructs 1–5 obtained at 10 M Ca^{2+}_i . *Different from cbv1 ($P < 0.05$); #Different from cbv1+h $\beta 1$ ($P < 0.05$). Error bars correspond to SEM; each point represents the average of ≥ 4 patches. doi:10.1371/journal.pone.0109306.g003

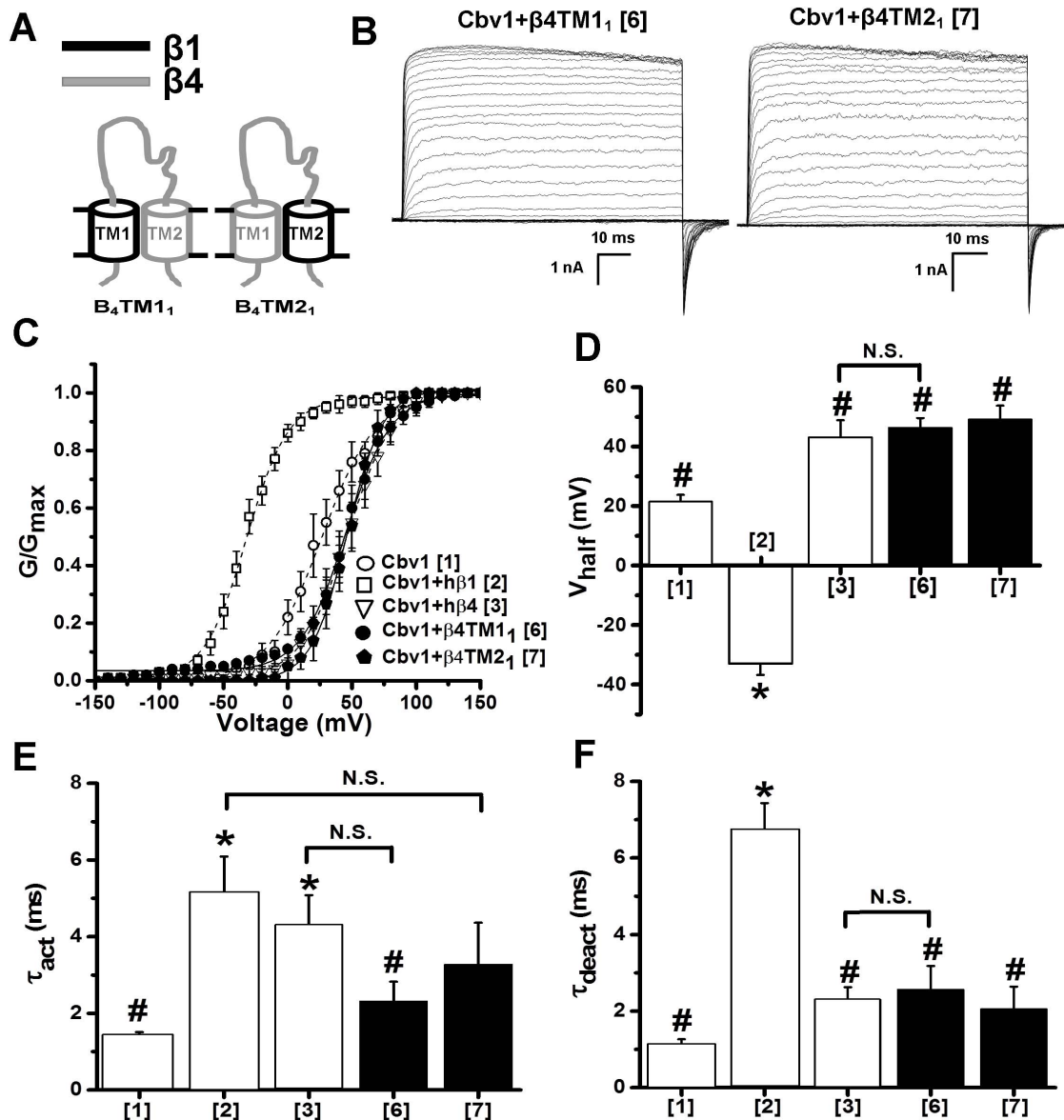


Figure 4. Neither TM1 or TM2 from BK $\beta 1$ is sufficient to confer the characteristic phenotype of $\beta 1$ -containing to BK channel complexes. (A) Cartoons depicting chimeric constructs that result from swapping individual transmembrane domains (either TM1 or TM2) between h $\beta 1$ and h $\beta 4$. Regions from $\beta 1$ and $\beta 4$ are given in black and grey, respectively. (B) Macroscopic current recordings obtained from I/O oocyte membrane patches expressing cbv1+ $\beta 4TM1_1$ (construct 6) or cbv1+ $\beta 4TM2_1$ (construct 7); $Ca^{2+}_i = 10 \mu M$. (C) Averaged G/G_{max} -V plots of cbv1, cbv1+h $\beta 1$, cbv1+h $\beta 4$, cbv1+ $\beta 4TM1_1$, and cbv1+ $\beta 4TM2_1$; $Ca^{2+}_i = 10 \mu M$. Averaged V_{half} (D), activation (E) and deactivation (F) time constants (τ_{act} , τ_{deact} respectively) obtained cbv1, cbv1+h $\beta 1$, cbv1+h $\beta 4$, cbv1+ $\beta 4TM1_1$ and cbv1+ $\beta 4TM2_1$; $Ca^{2+}_i = 10 \mu M$. *Different from cbv1 ($P < 0.05$); #Different from cbv1+ $\beta 1$ ($P < 0.05$). Error bars correspond to SEM; each point represents the average of ≥ 4 patches. doi:10.1371/journal.pone.0109306.g004

Finally, we decided to determine whether integrity in the peptidic connection between $\beta 1TM1$ and $\beta 1TM2$ *via* the EC loop was necessary to provide the normal phenotype of cbv1+h $\beta 1$ channels. Thus, we engineered two “split” chimeras from the $\beta 4TMs_1$ to render: 1) “N-half chimera”, which contained the N-terminus from $\beta 4$, TM1 from $\beta 1$ and proximal half of $\beta 4$ EC loop; 2) “C-half chimera”, which contained the distal half of $\beta 4$ EC loop, TM2 from $\beta 1$, and the C-terminus from $\beta 4$ (Fig. 5A). After oocyte co-injection of these two chimeras with cbv1, surface expression of both chimeras was confirmed by surface biotinylation (Fig. 5B). Electrophysiology data demonstrate that V_{half} - Ca^{2+}_i plots (Figs. 5C,D and S1D), τ_{act} (Fig. 5F) and τ_{deact}

(Fig. 5G) from the resulting cbv1+chimeric $\beta 1/\beta 4$ heteromers are not able to reproduce the cbv1+h $\beta 1$ phenotype (Fig. 3) but match those of homomeric cbv1 channels. These data indicate that co-expression of each $\beta 1$ TM surrounded by its “immediate” $\beta 4$ background (Fig. 5A) is not sufficient to render the characteristic cbv1+h $\beta 1$ channel phenotype. Rather, a physical connection between two individual $\beta 1TM1$ and $\beta 1TM2$ *via* the EC loop is necessary to ensure such phenotype.

Discussion

In spite of the significant advances in addressing the role of BK $\beta 1$ subunits in the different aspects of slo1 channel gating and in

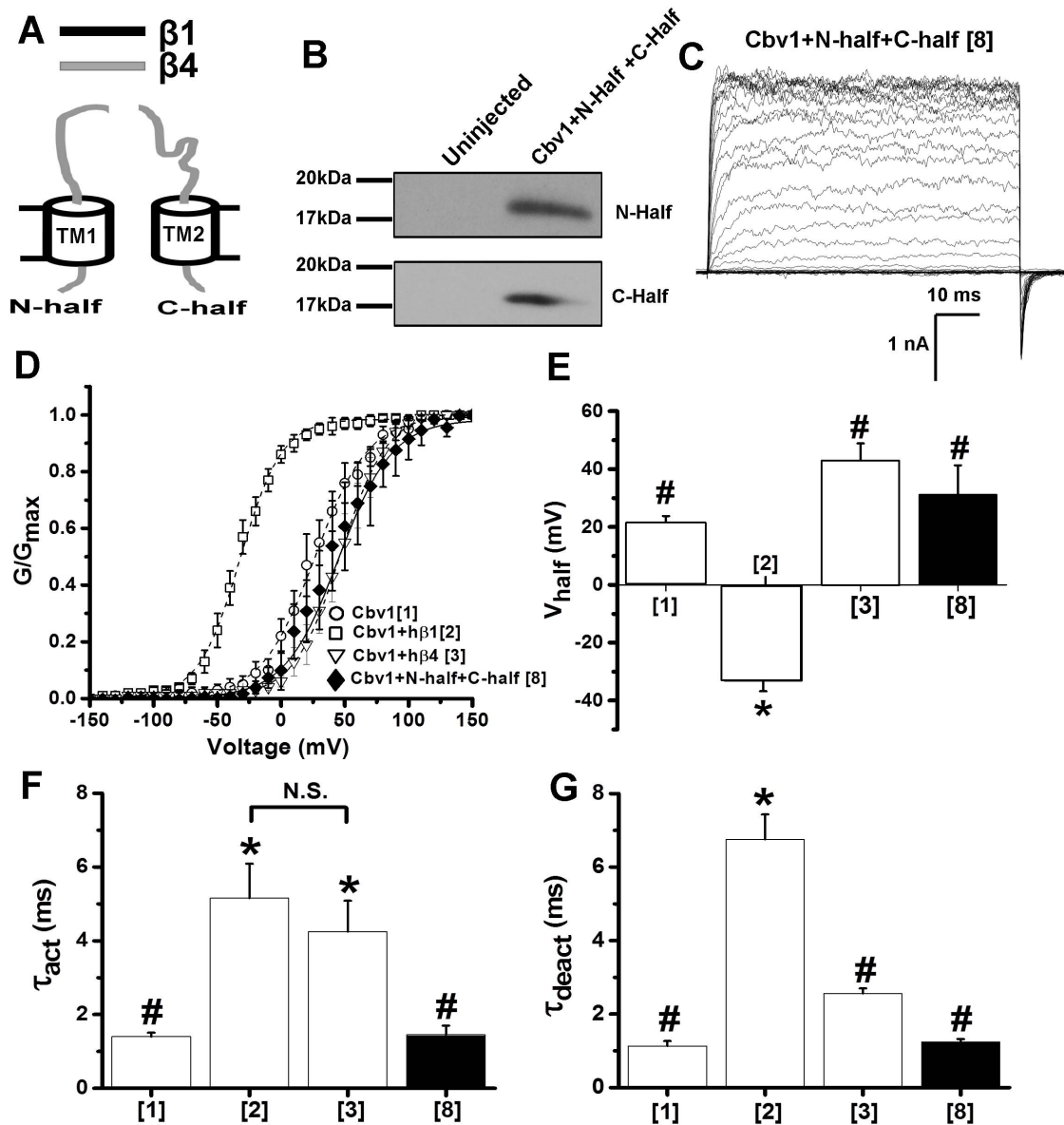


Figure 5. Physical continuity of the EC loop between TM1 and TM2 is essential to confer the characteristic phenotype of $\beta 1$ -containing BK channel complexes. (A) Cartoons depicting two h $\beta 1$ /h $\beta 4$ chimeric constructs termed “N-half” and “C-half”, obtained by cleaving the EC loop between TM1 and TM2 in the $\beta 4$ TM₁ chimera. Regions of $\beta 1$ and $\beta 4$ are given in black and grey, respectively. When expressed together (panels C-G and main text), “N-half” and “C-half” chimera have been labeled as construct 8. (B) Western blots reflecting the surface presence of N-half and C-half, when co-expressed with cbv1, obtained by surface biotinylation of *Xenopus* oocytes expressing cbv1+N-half+C-half complexes. Blot image where left and right lanes contain samples from uninjected and N-half+C-half chimera-injected oocytes, respectively. (C) Representative traces of macroscopic current recordings obtained from I/O oocyte membrane patches expressing construct 8; $Ca^{2+}_i = 10 \mu M$. (D) Averaged G/G_{max} -V plots from cbv1, cbv1+h $\beta 1$, cbv1+h $\beta 4$, and cbv1+construct 8; $Ca^{2+}_i = 10 \mu M$. (E) Averaged V_{half} (E), activation (F) and deactivation (G) time constants (τ_{act} , τ_{deact} respectively) obtained cbv1, cbv1+h $\beta 1$, cbv1+h $\beta 4$, and cbv1+construct 8. *Different from cbv1 ($P < 0.05$); #Different from cbv1+h $\beta 1$ ($P < 0.05$). Error bars show SEM; each point represents the average of ≥ 4 patches. doi:10.1371/journal.pone.0109306.g005

cell physiology and pathophysiology, the involvement of specific BK $\beta 1$ regions in determining the characteristic phenotype of $\beta 1$ -containing BK currents remains unresolved. A previous study has shown that the $\beta 1$ EC loop regulates intrinsic gating and voltage sensor activation. However, data fall short from demonstrating that the $\beta 1$ EC loop is sufficient to modulate the apparent Ca^{2+}_i sensitivity of the channel [24], a channel property that is critical for the role of $\beta 1$ -containing BK channels in cell function. On the other hand, studies from BK channels made of slo1 and chimeric $\beta 1/\beta 2$ subunits indicated that β C- and N-ends played a

significant role in determining the channel phenotype, and raised the hypothesis that β TMs contribute to overall functional coupling between α and β subunits [16]. Indeed, our current study clearly demonstrates that neither $\beta 1$ TM is sufficient but both are necessary to increase the channel's apparent Ca^{2+}_i sensitivity.

The current data also demonstrate that for both TMs to provide the basic phenotype of beta1-containing BK channels, these two segments must be physically connected, in this case *via* the EC loop of $\beta 4$ subunit. Noteworthy, EC loops from $\beta 1$ and $\beta 4$ share

two critical domains that determine V_{half} [24; see next paragraph]. At least two interpretations on this crucial role of an EC loop are possible: 1) the connection between the two TMs *via* the EC loop helps to properly orient both TMs, so each efficiently interacts with a corresponding slo1 functional domain partner. It is interesting to note that disulfide cross-linking assays placed the outer face of β 1 TM1 in close proximity to the outer faces of slo1 S1 and S2 domains while placing the outer face of β 1 TM2 in the vicinity of the outer face of S0 in the adjacent slo1 subunit [5,22,33]. If physical associations match functional coupling (yet restrictions are considered below), the EC loop physical's integrity would allow optimal β 1 TM1-slo1 S1/S2 and β 1 TM2-slo1 S0 functional coupling; 2) functional coupling between a single β 1 TM and its corresponding functional domain in slo1 is translated into modification of phenotype only if such functional coupling imparts a change in conformation/topology of the other β 1 TM, such communication between TMs requiring the physical integrity of the EC loop.

Previous studies on the role of EC loop of β 1 on BK/ β 1 channel modulation revealed two critical domains (A and B) in the EC loop that were important to modulate various functional parameters, such as V_{half} , τ_{act} , τ_{deact} and voltage sensitivity of β 1-containing BK channels [24]. Noteworthy, we engineered split chimeras so the N-half chimera contained the 'A' domain in its entirety whereas the C-half chimera contained the 'B' domain in its entirety (Fig. 5A). Our biotinylation data demonstrate that both the N-half and the C-half chimera were properly expressed in the cell membrane. However, neither chimera was sufficient to bring the phenotype of β 1-containing BK channels. Moreover, when both half-chimeras were coexpressed with *cbv1*, they failed to evoke the normal phenotype of β 1-containing BK channels. This failure can be explained by some non mutually exclusive possibilities: when physically separated from each other, the half-chimeras, while present in the membrane, failed to acquire the proper stoichiometry and/or conformational association with the channel-forming subunits [see above]. In synthesis, our results indicate that segments A and B *per se* are not sufficient to provide the normal phenotype of β 1-containing BK channels but a physical connection between the two β 1 halves is needed.

Remarkably, both BK β 1 and β 2 increase the channel's apparent calcium sensitivity to a similar degree [1,17]. We speculate that this similar change in phenotype recognizes a similar physical association between these regulatory subunits and slo1. Using a TOX-CAT assay, Morera et al. (2012) [34] have demonstrated a physical association between β 2 TM1 and slo1 S1 whereas physical interactions between slo1 and other β regions (EC loop, TM2) could not be observed. Our functional data, however, show that the β 1 N-half chimera, which includes TM1, while fully expressed in the membrane (Fig. 5B), failed to alter slo1 current phenotype. Thus, as previously documented by cysteine substitutions that alter slo1- β subunit physical association but not phenotype [35], physical association is not sufficient to document functional coupling between β and α BK subunits.

Our current data provide critical information over previous findings on the structural bases of BK channel function regulation by accessory subunits. Using chimeric channels made by swapping *mslo1/hlo1* and *dslo1* regions it has been shown that the slo1 N-end and S0 are both critical for channel function regulation by β 1 [4,21,35]. In addition, disulfide cross-linking studies have shown that the N-terminal EC end of slo1 S0 is in close proximity to its S3 and S4 segments. These three segments (S0, S3, S4) are thought to move in concert during voltage sensor activation [5,20].

Consequently, substitutions in S0 disrupt the voltage-dependent activation of BK channels, underscoring the critical role of S0 in channel function [36]. Disulfide cross-linking studies [5,20] show that BK β 1 TM1 and TM2 are both packed close to each other at the mouth of the cleft between the voltage sensing domain (VSD) of two adjacent slo1 [5,20]. Within this cleft, TM1 is close to S1 of one VSD and TM2 close to S0 of the adjacent VSD [5,20,22]. The proposed location of both TM1 and TM2 and our current data raise the hypothesis that β 1 TMs and slo1 VSD are functionally coupled within membrane-spanning regions themselves, the VSD serving as a scaffold for proper β 1 subunit conformation.

In conclusion, from a combination of patch-clamp electrophysiology on BK channels made of *cbv1* and native or chimeric β 1 subunits, and surface biotinylation, we demonstrate for the first time that both transmembrane domains of BK β 1 are required to provide the characteristic ion current phenotype of β 1-containing BK channels. Moreover, BK β 1 transmembrane regions need to be physically linked by the EC loop in order to control essential parameters of BK current, such as V_{half} , activation and deactivation kinetics. Current information will lead to pinpoint mutagenesis strategies to identify the specific amino acid residues that are involved in providing the phenotype of β 1-containing BK channels, which represents a first necessary step to understand how β 1 couples to channel-forming slo1 proteins and to design selective BK β 1-targeting agents and modify tissue physiology in a rather selective manner.

Supporting Information

Figure S1 Both TMs of BK β 1 subunit are required for conferring the characteristic phenotype (V_{half}) of β 1-containing BK channel complexes. Averaged $V_{\text{half}}\text{-Ca}^{2+}_i$ plots for constructs 1-8, obtained over a wide range of Ca^{2+}_i levels (nominal zero to 100 μM). (A) β 1-subunit (construct 2) causes an increase in the channel's apparent Ca^{2+} sensitivity (which is more evident at $>1 \mu\text{M}$ Ca^{2+}_i), whereas β 4 (construct 3) does not. (B) β 1/ β 4 chimera containing both TM domains from β 1 (construct 5) reproduces the characteristic phenotype (e.g. V_{half}) of β 1-containing BK channels over a wide range of Ca^{2+}_i , including physiological levels found nearby the BK channel during smooth muscle contraction. (C) Chimeras containing individual TM domains (TM1 and TM2) from β 1 (constructs 6 and 7) fail to mimic the $V_{\text{half}}\text{-Ca}^{2+}_i$ relationship of β 1-containing BK channels. (D) Cleaving the EC loop between TM1 and TM2 in the β 4TMs1 chimera (construct 8) also fails to reproduce the normal $V_{\text{half}}\text{-Ca}^{2+}_i$ relationship of BK β 1 channels. Error bars correspond to SEM; each point represents the average of ≥ 4 patches. (TIF)

Acknowledgments

Authors thank Anna Bukiya for valuable suggestions on surface biotinylation experiments and discussion, and Bangalore Shivakumar and Maria Asuncion-Chin (UTHSC) for construction of split chimeras and excellent technical assistance.

Author Contributions

Conceived and designed the experiments: GK AMD. Performed the experiments: GK. Analyzed the data: GK AMD. Contributed reagents/materials/analysis tools: LT. Wrote the paper: GK AMD. Edited the manuscript: LT.

References

- Orio P, Latorre R (2005) Differential effects of beta 1 and beta 2 subunits on BK channel activity. *J. Gen. Physiol.* 125, 395–411.
- Latorre R, Morera FJ, Zaelzer C (2010) Allosteric interactions and the modular nature of the voltage- and Ca^{2+} -activated (BK) channel. *J. Physiol.* 588, 3141–3148.
- Dopico AM, Bukiya AN, Singh AK (2012) Large conductance, calcium- and voltage-gated potassium (BK) channels: Regulation by cholesterol. *Pharmacol. Ther.* 135, 133–150.
- Wallner M, Meera P, Toro L (1996) Determinant for beta-subunit regulation in high-conductance voltage-activated and Ca^{2+} -sensitive K^+ channels: an additional transmembrane region at the N terminus. *Proc. Natl. Acad. Sci. U S A.* 93, 14922–14927.
- Liu G, Niu X, Wu RS, Chudasama N, Yao Y, et al. (2010) Location of modulatory beta subunits in BK potassium channels. *J. Gen. Physiol.* 135, 449–459.
- Semenova NP, Abarca-Heidemann K, Loranc E, Rothberg BS (2009) Bimane fluorescence scanning suggests secondary structure near the S3-S4 linker of BK channels. *J. Biol. Chem.* 284, 10684–10693.
- Pantazis A, Kohanteb AP, Olcese R (2010) Relative motion of transmembrane segments S0 and S4 during voltage sensor activation in the human BK_{Ca} channel. *J. Gen. Physiol.* 136, 645–657.
- Wei A, Solaro C, Lingle C, Salkoff L (1994) Calcium sensitivity of BK-type K_{Ca} channels determined by a separable domain. *Neuron.* 13, 671–681.
- Orio P, Rojas P, Ferreira G, Latorre R (2002) New disguises for an old channel: MaxiK channel beta-subunits. *News. Physiol. Sci.* 17, 156–161.
- Pérez GJ, Bonev AD, Nelson MT (2001) Micromolar Ca^{2+} from sparks activates Ca^{2+} -sensitive K^+ channels in rat cerebral artery smooth muscle. *Am. J. Physiol. Cell. Physiol.* 281, C1769–C1775.
- Brayden JE, Nelson MT (1992) Regulation of arterial tone by activation of calcium-dependent potassium channels. *Science.* 256, 532–535.
- Bao L, Cox DH (2005) Gating and ionic currents reveal how the BKCa channel's Ca^{2+} sensitivity is enhanced by its beta1 subunit. *J. Gen. Physiol.* 126, 393–412.
- Wang B, Brenner R (2006) An S6 mutation in BK channels reveals beta1 subunit effects on intrinsic and voltage-dependent gating. *J. Gen. Physiol.* 128, 731–744.
- Meera P, Wallner M, Jiang Z, Toro L (1996) A calcium switch for the functional coupling between alpha (hsl) and beta subunits ($\text{K}_{\text{V,Ca}}$ beta) of maxi K channels. *FEBS. Lett.* 382, 84–88.
- Cox DH, Aldrich RW (2000) Role of the beta1 subunit in large-conductance Ca^{2+} -activated K^+ channel gating energetics. Mechanisms of enhanced Ca^{2+} sensitivity. *J. Gen. Physiol.* 116, 411–432.
- Orio P, Torres Y, Rojas P, Carvacho I, Gracia ML, et al. (2006) Structural determinants for functional coupling between the beta and alpha subunits in the Ca^{2+} -activated K^+ (BK) channel. *J. Gen. Physiol.* 127, 191–204.
- Brenner R, Jegla TJ, Wickenden A, Liu Y, Aldrich RW (2000) Cloning and functional characterization of novel large conductance calcium-activated potassium channel beta subunits, hKCNMB3 and hKCNMB4. *J. Biol. Chem.* 275, 6453–6461.
- Valverde MA, Rojas P, Amigo J, Cosmelli D, Orio P, et al. (1999) Acute activation of Maxi-K channels (hSlo) by estradiol binding to the beta subunit. *Science.* 285, 1929–1931.
- Bukiya AN, Singh AK, Parrill AL, Dopico AM (2011) The steroid interaction site in transmembrane domain 2 of the large conductance, voltage- and calcium-gated potassium (BK) channel accessory β 1 subunit. *Proc. Natl. Acad. Sci. U S A.* 108, 20207–20212.
- Bukiya AN, Mcmillan JE, Fedinec AL, Patil SA, Millar DD, et al. (2013) Cerebrovascular dilation *via* selective targeting of the cholane steroid site in the BK channel β 1-subunit by a novel non-steroidal agent. *Mol. Pharmacol.* 83, 1030–1044.
- Lee US, Shi J, Cui J (2010) Modulation of BK channel gating by the β 2 subunit involves both membrane-spanning and cytoplasmic domains of Slo1. *J. Neurosci.* 30, 16170–16179.
- Wu RS, Chudasama N, Zakharov SI, Doshi D, Motoike H, et al. (2009) Location of the beta 4 transmembrane helices in the BK potassium channel. *J. Neurosci.* 29, 8321–8328.
- Wu RS, Liu G, Zakharov SI, Chudasama N, Motoike H, et al. (2013) Positions of β 2 and β 3 subunits in the large-conductance calcium- and voltage-activated BK potassium channel. *J. Gen. Physiol.* 141, 105–117.
- Gruslova A, Semenov I, Wang B (2012) An extracellular domain of the accessory β 1 subunit is required for modulating BK channel voltage sensor and gate. *J. Gen. Physiol.* 139, 57–67.
- Jaggar JH, Li A, Parfenova H, Liu J, Umstot ES, et al. (2005) Heme is a carbon monoxide receptor for large-conductance Ca^{2+} -activated K^+ channels. *Circ. Res.* 97, 805–812.
- Bukiya AN, Liu J, Dopico AM (2009) The BK channel accessory beta1 subunit determines alcohol-induced cerebrovascular constriction. *FEBS. Lett.* 583: 2779–2784.
- Dopico AM (2003) Ethanol sensitivity of BK_{Ca} channels from arterial smooth muscle does not require the presence of the beta 1-subunit. *Am. J. Physiol. Cell. Physiol.* 284, C1468–C1480.
- Glantz SA (2001) Primer of Biostatistics. New York: McGraw-Hill.
- Bukiya AN, Vaithianathan T, Toro L, Dopico AM (2008) The second transmembrane domain of the large conductance, voltage- and calcium-gated potassium channel beta1 subunit is a lithocholate sensor. *FEBS. Lett.* 582, 673–678.
- Horrigan FT, Aldrich RW (2002) Coupling between voltage sensor activation, Ca^{2+} binding and channel opening in large conductance (BK) potassium channels. *J. Gen. Physiol.* 120, 267–305.
- Contreras GF, Neely A, Alvarez O, Gonzalez C, Latorre R (2012) Modulation of BK channel voltage gating by different auxiliary β subunits. *Proc. Natl. Acad. Sci. U S A.* 109, 18991–18996.
- Nimigean CM, Magleby KL (2000) Functional coupling of the beta1 subunit to the large conductance Ca^{2+} -activated K^+ channel in the absence of Ca^{2+} . Increased Ca^{2+} sensitivity from a Ca^{2+} -independent mechanism. *J. Gen. Physiol.* 115, 719–736.
- Liu G, Zakharov SI, Yang L, Wu RS, Deng SX, et al. (2008) Locations of the beta1 transmembrane helices in the BK potassium channel. *Proc. Natl. Acad. Sci. U S A.* 105, 10727–10732.
- Morera FJ, Alioua A, Kundu P, Salazar M, Gonzalez C, et al. (2012) The first transmembrane domain (TM1) of β 2-subunit binds to the transmembrane domain S1 of α -subunit in BK potassium channels. *FEBS Lett.* 586: 2287–2293.
- Morrow JP, Zakharov SI, Liu G, Yang L, Sok AJ, et al. (2006) Defining the BK channel domains required for beta1-subunit modulation. *Proc. Natl. Acad. Sci. U S A.* 103: 5096–5101.
- Koval OM, Fan Y, Rothberg BS (2007) A role for the S0 transmembrane segment in voltage-dependent gating of BK channels. *J. Gen. Physiol.* 129, 209–220.